Two Novel Cyclopentadithiophene-Based Alternating Copolymers as Potential Donor Components for High-Efficiency Bulk-Heterojunction-Type Solar Cells

Adam J. Moulé,*[,†,‡] Argiri Tsami,[§] Torsten W. Bünnagel,[§,⊥] Michael Forster,[§] Nils M. Kronenberg,[†] Markus Scharber,[||] Markus Koppe,[||] Mauro Morana,[||] Christoph J. Brabec,[||] Klaus Meerholz,*[,†] and Ullrich Scherf*[,§]

Macromolecular Chemistry Group and Institute for Polymer Technology, Bergische Universität Wuppertal, Gauss-Strasse 20, D-42097 Wuppertal, Germany, Institut für Physikalische Chemie, Universität zu Köln, Luxemburger Strasse 116, D-50939 Köln, Germany, Konarka Austria GmbH, Altenbergerstrasse 69, A-4040 Linz, Austria, and Chemical Engineering and Materials Science, 1 Shields Avenue, University of California, Davis, California 95616

Received March 6, 2008. Revised Manuscript Received April 3, 2008

Polymer/fullerene bulk heterojunctions have recently generated a lot of scientific interest due to their potential in low-cost photovoltaic applications. In this paper we detail the synthesis and characterization of two new low-band-gap polythiophenes, poly[4,4-bis(2-ethylhexyl)-4*H*-cyclopenta[2,1-*b*:3,4-*b*′]dithiophene-2,6-diyl-*alt*-4,7-bis(2-thienyl)-2,1,3-benzothiadiazole-5′,5″-diyl] (PCPDTTBTT) and poly[4,4-bis(2-ethylhexyl)-4*H*-cyclopenta[2,1-*b*:3,4-*b*′]dithiophene-2,6-diyl-*alt*-2,3-dioctylquinoxaline-5,8-diyl] (PCPDTQ), for use in these applications. The PCPDTQ polymer did not produce efficient solar cells. A high power efficiency of 2.1% under one sun was found for a PCPDTTBTT/fullerene mixture. The high efficiency was achieved by alteration of the morphology using a solvent additive. Analysis of atomic force microscopy phase images shows that material phases with distinct mixing ratios are formed and altered with the addition of the solvent additive.

Introduction

Polymeric solar cells have received increasing attention from both academic and industrial laboratories due to their high charge-separation efficiency and ease of processing. Bulk-heterojunction-type solar cells use a phase-separated blend of an organic electron donor and an acceptor component. One of the most efficient donor components until now has been the semiconducting polymer poly(3-hexylthiophene) (P3HT) in combination with a soluble fullerene derivative (C_{61}-PCBM) as the nonpolymeric acceptor. However, the maximum power conversion efficiency (PCE) of this donor/acceptor couple is limited to ∼5% due to the incomplete match with the solar spectrum and the large offset of the LUMO energy levels of the donor and acceptor.[1–3]

Various lower band gap semiconducting donor polymers have been developed in recent years for a better match with the solar spectrum, especially in the 1.4−1.9 eV region. In particluar, so-called "donor/acceptor" (DA) alternating copolymers that contain alternating electron-rich and electron-poor building blocks have been favored.[1,4–10] The performance of bulk-heterojunction-type solar cells with an active layer of these DA copolymers and C_{61}-PCBM could, in principle, reach a 10% power conversion efficiency (PCE).[3] The PCE is mainly influenced by the morphology of the phase separated blends and the charge carrier mobility in the two phases.

Since reliable design rules for the synthesis and solid-state self-assembly behavior of such DA copolymers are still not available, the search for novel DA copolymers is mainly guided by the "trial and error" principle. In a molecular LEGO game, as many combinations as possible of available donor and acceptor building blocks are generated and subsequently characterized. The alternating connection of the building blocks is in most cases realized by aryl−aryl cross-coupling reactions, e.g., following the methods of Suzuki or Stille. In this search, alternating copolymers containing the

* To whom correspondence should be addressed. (A.J.M.) Phone: (530) 754-8669. Fax: (530) 752-1031. E-mail: amoule@ucdavis.edu. (K.M.) Phone: +49 0221-470-3275. E-mail: klaus.meerholz@uni-koeln.de. (U.S.) Phone: +49 0202-439-2493 (3871). Fax: 0202-439-3880. E-mail: scherf@uni-wuppertal.de.
† Universität zu Köln.
‡ University of California.
§ Bergische Universität Wuppertal.
|| Konarka Austria GmbH.
⊥ Current address. CDT Ltd., Greenwich House, Madingley Rise, Madingley Road, Cambridge, CB3, 0TX, U.K.

(1) Hoppe, H.; Sariciftci, N. S. *J. Mater. Chem.* **2006**, *16* (1), 45–61.
(2) Ma, W.; Yang, C.; Gong, X.; Lee, K.; Heeger, A. J. *Adv. Funct. Mater.* **2005**, *15*, 1617–1622.
(3) Scharber, M. C.; Wuhlbacher, D.; Koppe, M.; Denk, P.; Waldauf, C.; Heeger, A. J.; Brabec, C. L. *Adv. Mater.* **2006**, *18* (6), 789–794.
(4) Zhang, F. L.; Mammo, W.; Andersson, L. M.; Admassie, S.; Andersson, M. R.; Inganas, L.; Ingands, O. *Adv. Mater.* **2006**, *18* (16), 2169–2173.
(5) McNeill, C. R.; Abrusci, A.; Zaumseil, J.; Wilson, R.; McKiernan, M. J.; Burroughes, J. H.; Halls, J. J. M.; Greenham, N. C.; Friend, R. H. *Appl. Phys. Lett.* **2007**, *90* (19), No. 193506.
(6) Blouin, N.; Michaud, A.; Leclerc, M. *Adv. Mater.* **2007**, *19* (17), 2295.
(7) Zhou, Q. M.; Hou, Q.; Zheng, L. P.; Deng, X. Y.; Yu, G.; Cao, Y. *Appl. Phys. Lett.* **2004**, *84* (10), 1653–1655.
(8) van Mullekom, H. A. M.; Vekemans, J.; Meijer, E. W. *Chem.−Eur. J.* **1998**, *4* (7), 1235–1243.
(9) Edder, C.; Armstrong, P. B.; Prado, K. B.; Frechet, J. M. J. *Chem. Commun.* **2006**, (18), 1965–1967.
(10) Zhang, Q. T.; Tour, J. M. *J. Am. Chem. Soc.* **1998**, *120* (22), 5355–5362.

10.1021/cm8006638 CCC: $40.75
Published on Web 05/21/2008

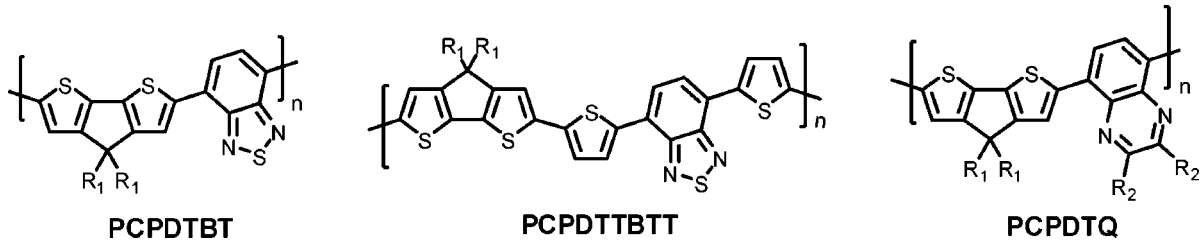

Figure 1. Chemical structures of the CPDT-based alternating DA copolymers PCPDTBT,[14] PCPDTTBTT, and PCPDTQ (R_1, R_2 = linear or branched alkyl).

Scheme 1. Synthesis of the CPDT-Based Alternating DA Copolymers PCPDTTBTT and PCPDTQ (R_1 = 2-Ethylhexyl, R_2 = *n*-Octyl) in Stille-Type Cross-Coupling Polycondensations

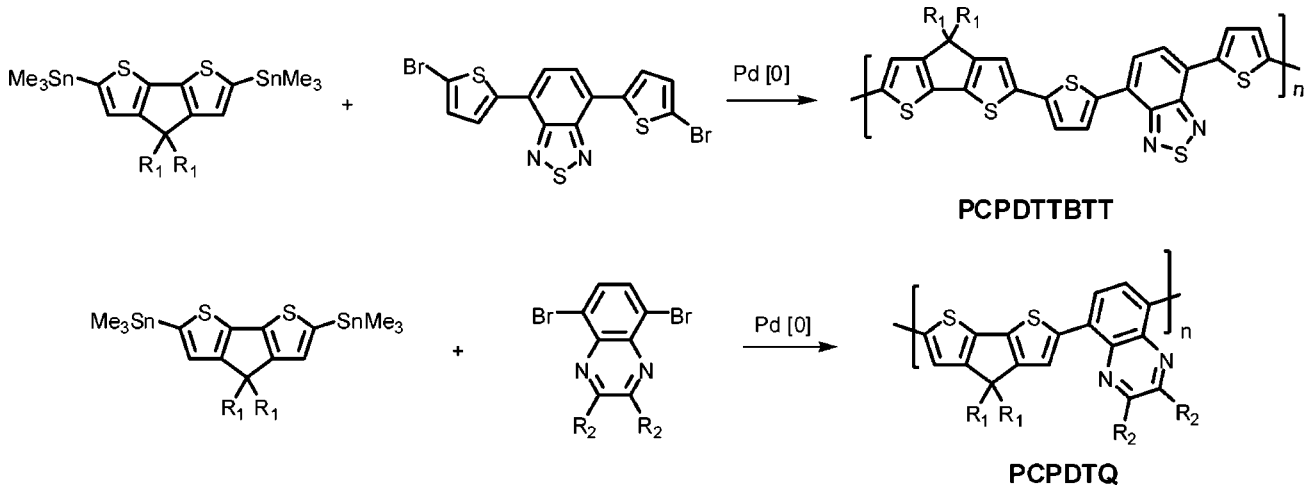

electron-rich 4,4-dialkyl-4*H*-cyclopenta[2,1-*b*:3,4-*b*′]dithiophene-2,6-diyl (CPDT) building block have come into the focus of interest. The synthesis of CPDT-type monomers and the resulting homopolymers has been previously described.[11,12] The novel alternating DA copolymer poly[4,4-bis(2-ethylhexyl)-4*H*-cyclopenta[2,1-*b*:3,4-*b*′]dithiophene-2,6-diyl-*alt*-2,1,3-benzothiadiazole-4,7-diyl] (PCPDTBT; see Figure 1), which combines the electron-rich CPDT (donor) building block with the 2,1,3-benzothiadiazole-4,7-diyl (TBT) acceptor unit, was recently introduced as a very promising donor component in bulk-heterojunction-type solar cells. In combination with the C_{61}-PCBM acceptor, a PCE of ca. 2.7% has been reported.[13] A further morphology optimization of the PCPDTBT/PCBM blend layers using a small amount of an alkylenedithiol additive led to the high efficiency of 5.5% in 2007 (obtained using C_{71}-PCBM).[14]

Experimental Section

We now describe two structurally related CPDT-based, alternating DA copolymers containing the 4,7-bis(2-thienyl)-2,1,3-benzothiadiazole-5′,5″-diyl or the 2,3-dialkylquinoxaline-5,8-diyl acceptor moiety. Poly[4,4-bis(2-ethylhexyl)-4*H*-cyclopenta[2,1-*b*:3,4-*b*′]dithiophene-2,6-diyl-*alt*-4,7-bis(2-thienyl)-2,1,3-benzothiadiazole-5′,5″-diyl] (PCPDTTBTT; see Figure 1)[15] and poly[4,4-bis(2-ethylhexyl)-4*H*-cyclopenta[2,1-*b*:3,4-*b*′]dithiophene-2,6-diyl-*alt*-2,3-dioctylquinoxaline-5,8-diyl] (PCPDTQ; see Figure 1) can be prepared with rather high mean average molar masses M_n of >13 000 g/mol in Stille-type cross-coupling reactions. Mean average molar masses of at least 10 000 g/mol seem necessary to obtain an optimum solid state ordering of the pure donor component and the copolymer/C_{61}-PCBM blend, though generally better performance has been seen with higher M_n, as least up to M_n values of roughly 30 000 g/mol depending on the polydispersity.[16] The novel DA copolymers, especially PCPDTTBTT showed rather promising power conversion efficiencies of up to ca. 2.1% in the first device experiments (bulk-heterojunction-type solar cells with copolymer/C_{61}-PCBM blends as the active layer), although the processing conditions and the morphology of the blends had not been optimized. The optimization of the solid-state structure and the blend morphology are the focus of ongoing investigations, e.g., the development of suitable processing and postprocessing protocols.

Synthesis. The synthesis of the two DA copolymers PCPDTTBTT and PCPDTQ with R_1 = 2-ethylhexyl and R_2 = *n*-octyl was accomplished in a Stille-type heteroaryl−heteroaryl cross-coupling, involving the reaction of 2,6-distannylated 4,4-dialkyl-CPDT[13] with the corresponding 5,5″-dibromo-4,7-bis(2-thienyl)-2,1,3-benzothiadiazole or 5,8-dibromo-2,3-dioctylquinoxaline[17] monomers (see Scheme 1). Further details of the synthesis and characterization of PCPDTTBTT and PCPDTQ can be found in the Supporting Information.

The resulting molar masses M_n and M_w of the DA copolymers are reported in Table S1 in the Supporting Information, together with the solution and solid-state optical properties (absorption,

(11) Asawapirom, U.; Scherf, U. *Macromol. Rapid Commun.* **2001**, *22* (10), 746–749.
(12) Coppo, P.; Turner, M. L. *J. Mater. Chem.* **2005**, *15* (11), 1123–1133.
(13) Muhlbacher, D.; Scharber, M.; Morana, M.; Zhu, Z. G.; Waller, D.; Gaudiana, R.; Brabec, C. *Adv. Mater.* **2006**, *18* (22), 2931–2931.
(14) Peet, J.; Kim, J. Y.; Coates, N. E.; Ma, W. L.; Moses, D.; Heeger, A. J.; Bazan, G. C. *Nat. Mater.* **2007**, *6* (7), 497–500.
(15) Jayakannan, M.; Van Hal, P. A.; Janssen, R. A. J. *J. Polym. Sci., Part A: Polym. Chem.* **2002**, *40* (2), 251–261.
(16) Schilinsky, P.; Asawapirom, U.; Scherf, U.; Biele, M.; Brabec, C. J. *Chem. Mater.* **2005**, *17* (8), 2175–2180.
(17) Tsami, A.; Bunnagel, T. W.; Farrell, T.; Scharber, M.; Choulis, S. A.; Brabec, C. J.; Scherf, U. *J. Mater. Chem.* **2007**, *17* (14), 1353–1355.

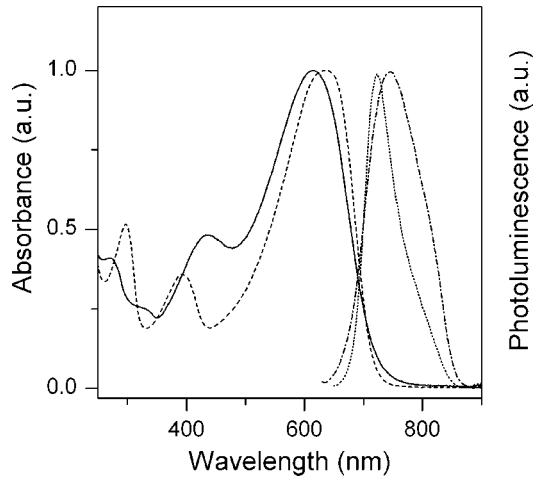

Figure 2. Solution absorption and emission spectra of the alternating DA copolymers PCPDTTBTT (solid and dashed−dotted, respectively) and PCPDTQ (dashed and dotted, respectively) (excitation 620 nm (PCPDTTBTT) and 650 nm (PCPDTQ), solvent chloroform).

photoluminescence). Figure 2 depicts the solution absorption and photoluminescence (PL) spectra of the alternating DA copolymers PCPDTTBTT and PCPDTQ. Both DA copolymers display two absorption maxima in the UV/vis region (see Table S1). The long wavelength absorption maximum $\lambda_{max,abs}$ of PCPDTTBTT is centered at 615 nm, that of PCPDTQ at 632 nm. The corresponding PL emission maxima $\lambda_{max,em}$ occur at 749 nm (PCPDTTBTT) and 722 nm (PCPDTQ). Both copolymers show rather similar absorption and emission spectra in dilute solution. The somewhat broader absorption band and blue-shifted absorption maximum of PCPDTTBTT may reflect a slightly increased conformational disorder due to the higher relative content of flexible aryl−aryl single bond connections in the repeat unit. The slightly increased conformational disorder of PCPDTTBTT in solution also causes the increased Stokes loss for this copolymer.

The solid-state absorption bands are red-shifted by 81 nm (PCPDTTBTT; see Figure S1) and 52 nm (PCPDTQ, not shown) for thin films spin-coated from a chlorobenzene solution. The higher wavelength solid-state absorption maximum of PCPDTTBTT (696 nm) relative to that of PCPDTQ (678 nm) reflects the slightly reduced optical band-gap energy for PCPDTTBTT, in full agreement with an extrapolation of the long-wavelength absorption edges of the solution UV/vis spectra. Also shown is a UV/vis spectrum of a PCPDTTBTT nanoparticle suspension. In P3HT, a nanoparticle suspension was shown to give the UV/vis spectrum that has the most crystalline configuration. Since the thin film and nanoparticle suspension have identical spectra, we can assume that this configuration represents the maximally aggregated and red-shifted configuration of PCPDTTBTT. Very little vibronic character can be seen in the solid-state UV/vis spectrum, which indicates that this polymer does not form extended crystalline domains. The ability to control the solid-state arrangement of the DA copolymers and the morphology of the donor/acceptor network is critical to optimizing the efficiency of the resulting bulk-heterojunction-type solar cells.

Device Fabrication and Characterization. All of our devices were fabricated on an indium tin oxide (ITO) coated substrate with a 40 nm layer of PEDOT/PSS spin-coated on top. The ITO and PEDOT/PSS were processed as previously reported.[18] The active layers were spin-coated from well-dissolved solutions in various

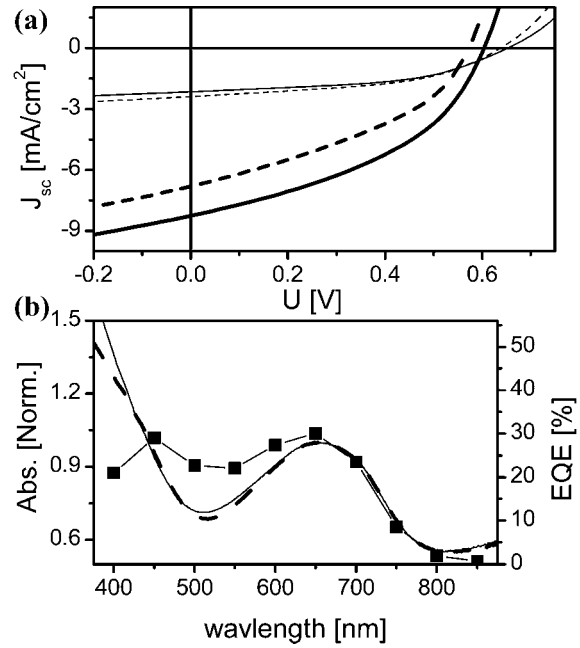

Figure 3. (a) $I-V$ curves of bulk-heterojunction-type solar cell devices cast from 1:3 (w/w) PCPDTTBTT/PCBM mixtures in CB (dashed bold; V_{oc} = 0.56 V, FF = 0.39, PCE = 1.5%) or CB/Ani (solid bold; V_{oc} = 0.60 V, FF = 0.42, PCE = 2.1%) and a 1:3 (w/w) PCPDTQ/PCBM mixture in CB (dashed; V_{oc} = 0.64 V, FF = 0.48, PCE = 0.74%) or CB/Ani (solid; V_{oc} = 0.60 V, FF = 0.42, PCE = 0.67%). All samples were measured as-cast. (b) UV/vis spectra and EQE of the CB-cast PCPDTTBTT-based devices shown in (a).

solvents. A Ca/Ag electrode was evaporated on top of the active layer. Seven devices were fabricated onto each substrate. The measured results from these devices were averaged for each substrate. All device fabrication and measurements were performed in N_2 gloveboxes. After fabrication, the devices were measured under simulated sunlight provided by a filtered Xe lamp to give an AM1.5 spectrum at 100 mW/cm.^{2} The lamp intensity was measured using a calibrated solar cell provided by the Fraunhofer Institute for Solar Cell Research (ISC). No mismatch factor was included in the calculation of the efficiency. EQE measurements were performed by filtering the same Xe lamp using Mellis Griot interference filters with an fwhm of 10 nm. The light intensity was calibrated using a Newport 1830-C optical power meter. Atomic force microscopy (AFM) was performed using a Surface Imaging System (SIS) Pico Station atomic force microscope with phase measurement capability.

Results and Discussion

We tested the two novel DA copolymers as donor components (with the acceptor C_{61}-PCBM) of bulk-heterojunction-type solar cells. The $J-V$ characteristics of the cells are depicted in Figure 3. The devices cast from the PCPDTTBTT polymer show a much higher short circuit density (J_{sc}) and PCE than the devices cast from the PCPDTQ polymer. Since the devices display very similar open circuit voltages (V_{oc}) and band gap (see Figure 2), it can be assumed that this difference does not arise from differences in the electrochemical HOMO and LUMO levels of the copolymers.[3] Measurement of the hole mobilities (μ_h) of the two copolymers (see the Supporting Information for experimental details) in an OFET configuration shows that PCPDTTBTT has the higher μ_h of 2×10^{-4} cm^2/(Vs)

(18) Moulé, A. J.; Bonekamp, J. B.; Meerholz, K. *J. Appl. Phys.* **2006**, *100*, 094503.

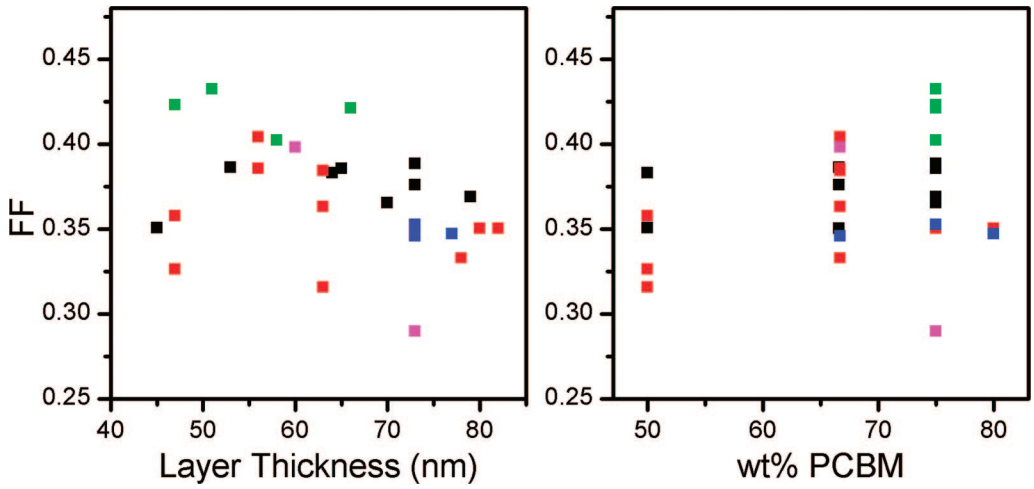

Figure 4. Filling factor for all of the PCPDTTBTT/PCBM PV devices fabricated in this study as functions of the active layer thickness (left) and [PCBM] (wt %) (right). The casting solvent used is represented by color: chlorobenzene (black), *o*-xylene (red), chlorobenzene + anisole (green), *o*-xylene + anisol (blue), and chlorobenzene + nitrobenzene (magenta). Each point represents 4−7 devices on the same substrate that have been averaged.

compared with a 1×10^{-4} cm^2/(Vs) for PCPDTQ. This difference in hole mobility does not, however, account for the large differences in J_{sc} between the two devices.[19] We find instead that a poorer device morphology is responsible for this difference. Since we wish to produce the highest efficiency PV devices possible, we focus the rest of this paper on the higher efficiency PCPDTTBTT polymer. A more careful look at the effects that device morphology can have on the performance of polymer/PCBM bulk-heterojunction solar cells is done for the PCPDTTBTT/PCBM devices.

We fabricated a series of PCPDTTBTT/PCBM devices with a range of mixing ratios and cast from different solvents and solvent mixtures, which has been shown to have a large effect on the morphology of P3HT-based solar cells.[20,21] For this study we used *o*-xylene (OX) and chlorobenzene (CB) as base solvents and altered the morphological properties of the films by adding nitrobenzene (NtB) or anisole (Ani) to the base solvents (see Figure 4). The best device was cast from 95% CB and 5% Ani (see Figure 3a). This device shows an improved J_{sc} and filling factor (FF) when compared with all of the other devices and has a high PCE of 2.1% under AM1.5 illumination at 100 mW/cm^2. Comparison of the UV/vis spectra of the CB- and CB/Ani-cast devices showed no differences for wavelengths longer than 600 nm and very little difference in the rest of the spectrum (see Figure 3b). The EQE of the CB-cast device closely mirrors the UV/vis spectrum with a maximum of 33% at ∼650 nm and a measurable EQE beyond 800 nm. For wavelengths shorter than 450 nm, the EQE is reduced due to absorption by the PEDOT/PSS electrode.

When a small (∼100 mg) quantity of a new material is being investigated for use in bulk-heterojunction solar cells, it is necessary to determine the effect of various fabrication parameters on the device performance. The most important of these parameters are the layer thickness, the ratio (wt %) of polymer to PCBM, the choice of casting solvent, and whether and at what temperature heat treatment is needed. For this study we were able to fabricate a total of 28 PCPDTTBTT/PCBM substrates with seven devices on each substrate. The fabrication conditions were chosen to determine which of the parameters listed above were most important for increasing the device efficiency.

In Figure 4, the FF for all 28 substrates is displayed as 2D plots of layer thickness (left) and [PCBM] (wt %) (right) with differences in casting solvent displayed in color. The full $J-V$ characteristics and discussion are presented in the Supporting Information (see Figure S2). The results for the FF were strongly dependent on the casting solvent. The FF was between 0.34 and 0.40 for all casting solvents except for the CB/Ani mixture (green). These devices showed an FF of 0.40−0.44. An improved FF in bulk-heterojunction devices occurs as a result of improved charge transport, typically due to an improved morphology.[1] A CB/Ani device had the highest efficiency of 2.1%. Comparison with devices cast from CB that had the same thickness and [PCBM] (wt %) showed that both an increased FF and an increased J_{sc} contribute to the increased PCE.

Overall, devices cast from OX performed the same as devices cast from CB in all categories. However, OX/Ani mixtures did not show an improved FF or efficiency. NtB has been shown to increase the as-cast efficiency of P3HT/PCBM devices by assisting the formation of polymer networks and nanoparticles.[22] However, the inclusion of NtB in the casting solvent led to a decrease in V_{oc}, FF, and J_{sc} for the PCPDTTBTT/PCBM devices shown here. The addition of NtB caused the formation of larger polymer domains in a sample with domains that were already larger than optimal (see Figure 5).[22] We therefore conclude that PCPDTTBTT already forms large pure particles without the addition of NtB to the casting solvent and the addition of NtB increases the size of the polymer domains to the detriment of device performance. In fact, the observation that

(19) Melzer, C.; Koop, E. J.; Mihailetchi, V. D.; Blom, P. W. M. *Adv. Funct. Mater.* **2004**, *14* (9), 865–870.
(20) Chang, J. F.; Sun, B. Q.; Breiby, D. W.; Nielsen, M. M.; Solling, T. I.; Giles, M.; McCulloch, I.; Sirringhaus, H. *Chem. Mater.* **2004**, *16* (23), 4772–4776.
(21) Rispens, M. T.; Meetsma, A.; Rittberger, R.; Brabec, C. J.; Sariciftci, N. S.; Hummelen, J. C. *Chem. Commun.* **2003**, (17), 2116–2118.
(22) Moulé, A. J.; Meerholz, K. *Adv. Mater.* **2008**, *20* (2), 240–245.

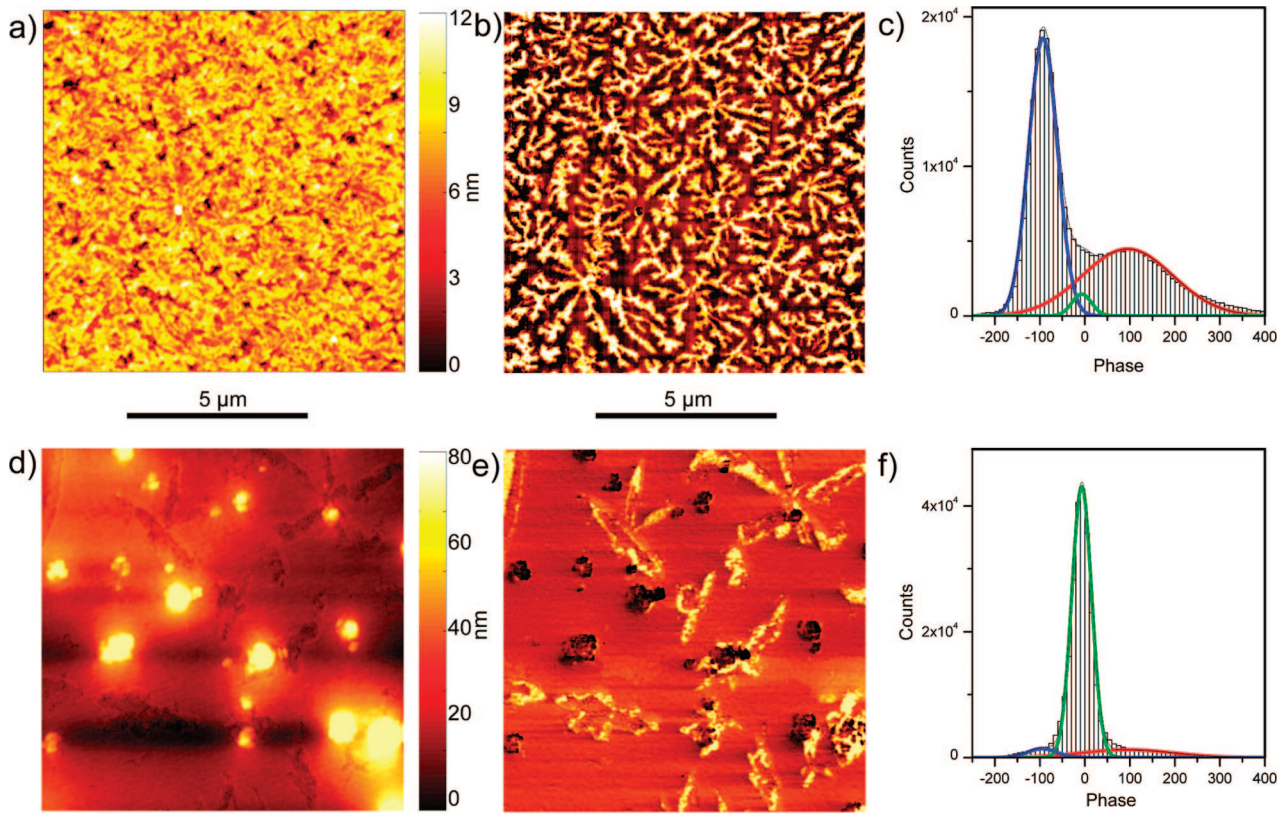

Figure 5. AFM topography and phase images of as-cast 1:3 (w/w) PCPDTTBTT/PCBM layers cast from CB (a, b) and CB/Ani (d,e). Histograms of the phase data for the CB-cast (c) and CB/Ani-cast (f) samples. The histograms have Gaussian fits to the PCBM-rich (blue), mixed (green), and PCPDTTBTT-rich (red) distributions.

Ani addition did increase the FF and NtB addition decreased the FF shows that solvent polarity regulates the layer morphology. The polarity of the solvent molecules increases in the order Ani < CB < NtB, which suggests that PCPDTTBTT is simply more soluble in lower polarity solvents. If this were true, we would expect that the average domain size would decrease with the addition of Ani.

In P3HT/PCBM bulk-heterojunction solar cells, the device efficiency is improved by using a postproduction heat treatment step[2] or high-boiling-point-solvent soaking.[23] These treatments led to reduced efficiency in the PCPDTTBTT/PCBM-cast devices (reduced V_{oc} and J_{sc}). We used AFM to determine why these treatments did not improve the device efficiency. Depicted in Figure 5a,b are topography and phase images of the CB-cast device with no heat treatment. It is clear from the phase image that the polymer and PCBM separate on a length scale of ~500 nm, which has been shown to reduce the performance of bulk-heterojunction solar cells[1] because the exciton diffusion length is much smaller, ~10 nm.[24] Since all of the postproduction treatments listed above cause an increase in the average domain size, they cause a reduction of the PCE in these devices. From this very coarse phase separation it is expected that the FF and efficiency of the device are very poor. Since the FF and efficiency of the CB/Ani device are both higher, we expected to observe a reduction in the average domain size in the AFM images. Parts d and e of Figure 5 show the topography and phase images, respectively, of the CB/Ani-cast device. Contrary to expectation, the CB/Ani-cast devices show both a greater surface roughness and a larger domain size than the CB-cast devices.

The phase image of the non-heat-treated CB/Ani device (see Figure 5e) shows three distinct feature types: first, a large dark-colored agglomerate, which is assigned to a PCPDTTBTT-rich phase; second, the leaflike lightly colored domains, which are assigned to a PCBM-rich phase; third, a background with an intermediate color. The leaflike domains have been previously reported for other polymer/PCBM mixtures.[25] We believe that the addition of a third, intermediate, phase takes place as a result of the addition of anisole to the CB base solvent.

To support our claim that the addition of anisole to the spin-casting mixture leads to the formation of a new mixed PCPDTTBTT/PCBM phase in the film, we examine the AFM phase data from Figure 5b,e in the form of histograms (see parts c and f, respectively, of Figure 5). The phase information seen in Figure 5b for the CB-cast film shows what appears to be a two-phase mixture. The corresponding histogram has two distinct peaks at different phase values, which indicate two main material features that we will call PCBM-rich and PCPDTTBTT-rich. These peaks were fit to Gaussian distributions. To completely fit the histogram line

(23) Li, G.; Shrotriya, V.; Huang, J.; Yao, Y.; Moriarty, T.; Emery, K.; Yang, Y. *Nat. Mater.* **2005**, *4*, 864–868.
(24) Markov, D. E.; Amsterdam, E.; Blom, P. W. M.; Sieval, A. B.; Hummelen, J. C. *J. Phys. Chem. A* **2005**, *109* (24), 5266–5274.
(25) Chirvase, D.; Parisi, J.; Hummelen, J. C.; Dyakonov, V. *Nanotechnology* **2004**, *15* (9), 1317–1323.

shape, a third distribution at an intermediate phase value had to be introduced; this we will call the mixed phase.

Since the average feature size of the CB-cast sample is ~500 nm and the layer thickness is only ~70 nm, it is a reasonable assumption that the surface features represent the phase separation for the entire layer. PCBM is 75 wt % in this layer. The integrated ratio of the PCBM-rich phase to the mixed phase to the PCPDTTBTT-rich phase Gaussian fit is 55.5:2.8:41.7 for the CB-cast film. The AFM phase data from the CB/Ani sample in Figure 5e were also converted into a histogram in Figure 5f and fit with three Gaussian distributions that had the same average phase values and standard deviations around these phase values, but with different integrated ratios. The integrated ratio of the PCBM-rich phase to mixed phase to PCPDTTBTT-rich phase Gaussian fit is 4.3:84.7:11.0. Since the phase values and standard deviations of the phase values are identical to those from the CB data, it can be reasonably assumed that the three distributions represent the same three mixing ratios in both phase images. The addition of 5% anisole to the spin-casting solvent clearly caused the formation of the mixed phase and a great reduction of the presence of the PCBM-rich and PCPDTTBTT-rich phases.

Further analysis allows the concentration limits for the three phases can be calculated. Assuming that the surface is flat (as seen in the topography image, this is a simplistic assumption), the upper limit for the PCPDTTBTT concentration in the PCPDTTBTT-rich and mixed phases can be fixed. The procedure is to assume that the PCBM-rich phase is actually 100% PCBM. The remaining PCBM is then distributed in the other two phases. Since we have two histograms and two components, four linear equations with four unknowns can be solved to give the upper limit concentrations listed in Table 1.

The addition of anisole to the casting solvent supports the growth of a phase with a concentration ratio intermediate between those of the two dominant phases of the CB-cast sample. This intermediate phase is responsible for the increased FF and efficiency of the CB/Ani-cast devices. Even with the improved CB/Ani-cast device, the FF and morphology are not ideal. The large PCBM-rich domains could carry dark current across the active layer, leading to reduced FF and PCE. However, experiments in which the anisole concentration of the casting solvent was increased beyond 5% led to a greatly reduced layer thickness, due to the lower viscosity of the solutions. More work is necessary to determine whether significant improvements to the FF can be made for this material mixture using improved morphology.

Table 1. Calculated Volume Percentages of Surface Coverage for the PCPDTTBTT-Rich, Mixed, and PCBM-Rich Phases and Weight Percentage Limits for PCPDTTBTT and PCBM in Each of the Three Phases[a]

	surface coverage (CB), vol %	surface coverage (CB/Ani), vol %	[PCPDTTBTT], wt %	[PCBM], wt %
PCPDTTBTT-rich phase	41.7	11.0	≤58	≥42
mixed phase	2.8	84.7	≤22	≥78
PCBM-rich phase	55.5	4.3	≥0	≤100

[a] These numbers are consistent for both casting solvents.

Conclusions

We report on the fabrication of two low-band-gap copolymers that have been designed for use in bulk-heterojunction-type solar cell devices. Devices fabricated from mixtures of PCPDTTBTT and PCBM show a promisingly high power efficiency of 2.1% with a measurable EQE for wavelengths longer than 800 nm. The devices were fabricated from a number of casting solvents. The use of a 19:1 (v/v) mixture of chlorobenzene and anisole gave the best performance. Analysis of the morphology showed that all devices had a very large phase separation, which can be expected to reduce the efficiency of the devices. The addition of anisole to the chlorobenzene casting solvent resulted in the formation of larger PCPDTTBTT-rich and PCBM-rich domains, but also in the formation of an intermediate mixed concentration domain that had superior electrical properties. This intermediate concentration domain led to an improved FF and efficiency. We recommend further testing of these polymers with the goal of finding fabrication conditions that improve the mixing of the polymer and fullerene components.

Acknowledgment. We thank the German Ministry of Science and Education (BMBF) for funding the EKOS project (Grant O3N2023D) and the Ministry of Science and Innovation of Northrhine-Westfalia (Elena-project).

Supporting Information Available: Experimental details, Figures S1 and S2, and Table S1 (PDF). This information is available free of charge via the Internet at http://pubs.acs.org.

CM8006638